LOCOMOTION ON SOFT GRANULAR SOILS: A DISCRETE ELEMENT BASED APPROACH FOR SIMULATIONS IN PLANETARY EXPLORATION

Roy Lichtenheldt and Bernd Schäfer

German Aerospace Center (DLR), Robotics and Mechatronics Center, Germany, Email: Roy.Lichtenheldt@dlr.de

ABSTRACT

To meet the increasing mobility demands in planetary exploration, there is a need for further detailed soil interaction models. Therefore a simulation framework based on the three-dimensional Discrete Element Method (DEM) is developed. This approach implicitly covers the soils grain relocation and the resulting plastic deformations. The model and framework are designated to predict the dynamic interaction with soft soils for development of locomotion equipment and strategies. As the shear strength of granular matter strongly depends on interparticle friction and rotation, a new interparticle contact model is developed. For determining the particle's contact parameters, a first procedure without the need of preliminary calibration simulations has been designed. First results, which could be used for wheel development are presented. Bevameter measurements are used to set the particles parameters as well as for verification issues.

Key words: Discrete Element Method; terramechanics; planetary rover; soil interaction;.

1. INTRODUCTION

Due to the increasing interests of science exploration on planets and moons, there is a need to extend the mobility performance of planetary exploration vehicles. The locomotion capabilities of these systems strongly depend on the interaction with soft granular soils. Thus a major design challenge is to develop suitable solutions for locomotion equipment and strategies. The mastering of these challenges depends on detailed soil interaction models to predict the system behaviour and get a better understanding of the underlying effects.
Due to the last years fast development of computation hardware, methods like Finite or Discrete Element Method (DEM) became computationally affordable in the field of terramechanics. Methods like Finite Element Method (FEM) or empirical models ([2], [3]) treat granular soils as continua. For discretisation meshes with fixed neighbored nodes are used. Therefore problems concerning distorted meshes due to large deformations may occur. Henceforth material transport is modeled as deformation of the continuum.
Most empirical models are based on Bekker's theory developed back in the 1960's ([2]). These models are usually based on a nonlinear dependency between pressure and sinkage of wheels, using additional terms to model the shear part of the deformation. These regularly do not cover the relocation of soil due to its deformation. A model using Bekker's theory in three dimensions and an additional procedure to model soil relocation is shown in [5]. Finite Element models as applied in [4] or [6] are mostly using Drucker-Prager model with Cap Plasticity. The soil is modeled using eulerian elements.
The Discrete Element approach features modeling of soft sandy soils on grain scale, thus the macroscopic soil deformation is based on interparticle contact reactions. As a result of this microscale modeling approach many effects, like plastic deformation due to grain relocation, are implicitly covered by the model. Furthermore the usage of discrete particles enables an insight to the effects of soil deformation (Figure 1).

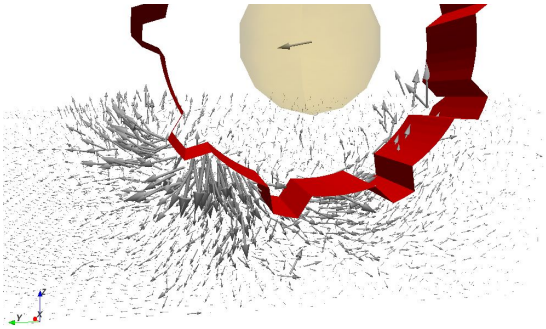

Figure 1. An insight to soil behaviour and deformation under dynamic loads: soil velocity fields below a driving wheel

Due to the particle based approach it is possible to set gravity as an input parameter concerning not only the wheel, but the soil density and shear strength, too.
The paper will focus on a newly developed wheel-soil interaction model and simulation framework based on the DEM simulator Pasimodo [1]. The model and framework are designated to predict the dynamic interaction with soft soils for development of locomotion equipment and strategies, supporting the increasing mobility demands.

2. DEM MODELING

2.1. Introduction

The Discrete Element Method has been first announced by Cundall & Strack [8] in 1979. It is based on modeling a granular medium from discrete particles without any fixed neighboring relation, thus the particles are free to move and contact each other in 6 DoF. Each particle's motion is then calculated out of the occurring contact forces. Thus the DEM does not need a mesh for discretisation of the medium.

Discrete Element Method has a wide range of applications, like in mining applications (conveyors and mills), excavation processes [9], [10], [11], [12], [13], rock mechanics [22], civil engineering [23] and geomechanics [24]. Wheel-soil interaction studies have been carried out in [18], [19], [20], [17], [21], [15], [16]. The approaches described in [15] and [16] are the only ones that cover three dimensions.

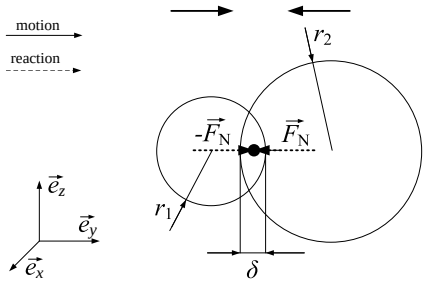

Figure 2. Soft particle contact generating overlap

The motion states for each particle can be obtained by integration of the principles of linear and angular momentum:

$$m\ddot{\vec{u}}_i = \sum \vec{F}_i^{\mathrm{C}} \tag{1}$$

$$J_i\ddot{\vec{\phi}}_i = \sum \vec{M}_i^{\mathrm{C}} \tag{2}$$

$$i \in [1,3]$$

whereat $\vec{F}_i^{\mathrm{C}}$ are the contact forces in direction $\vec{e}_i$, $\vec{M}_i^{\mathrm{C}}$ are the contact torques and J_i the moment of inertia in axis of rotation $\vec{e}_i$. Based on Figures 2 and 3 the contact reactions in normal direction can be calculated from the particles overlap δ and relative velocity $\dot{\vec{u}}_{mn}$ (Eq. 3, 4). Therefore a spring-damper element is assigned between the contacting particles m and n if $\delta > 0$. To keep the overlap as low as possible, a nonlinear elastic force $\vec{F}_{\mathrm{n}}^{c}$ correspondent to Hertzian theory and a damping force $\vec{F}_{\mathrm{n}}^{k}$ are applied in normal direction:

$$\vec{F}_{\mathrm{n}}^{c} = \frac{2E}{3(1-\nu^2)} \cdot \sqrt{r_{12} \cdot \delta_{mn}^3} \cdot \vec{n}_0 \tag{3}$$

$$\vec{F}_{\mathrm{n}}^{k} = \dot{u}_{mn} \cdot k_{\mathrm{n}} \cdot \vec{n}_0 \tag{4}$$

where r_{12} is the mean radius and $\vec{n}_0$ is the contact normal of the contacting particles m and n.

In tangential direction another spring-damper element is used to model the reaction forces up to the Mohr-Coulomb yield criterion. If the criterion is met, then the slider element is restricting the force to sliding friction. Therefore the tangential force $\vec{F}_{\mathrm{T}}$ could be calculated as follows:

$$\vec{F}_{\mathrm{T}} = \begin{cases} c_{\mathrm{T}} \cdot \vec{\delta}_{\mathrm{T}} & \forall \quad \vec{F}_{c\mathrm{T}} \leq F_{\mathrm{N}} \cdot \tan(\phi_{\mathrm{h}}) \\ \vec{F}_{\mathrm{N}} \cdot \tan(\phi_{\mathrm{g}}) & \forall \quad \vec{F}_{c\mathrm{T}} > F_{\mathrm{N}} \cdot \tan(\phi_{\mathrm{h}}) \end{cases} \tag{5}$$

where $\vec{\delta}_{\mathrm{T}}$ and c_{T} are the deflection and stiffness of the spring (Figure 3) and F_{N} is the total contact normal force of the particles m and n. ϕ_{h} and ϕ_{g} are the internal stick and slip friction angles. In addition to these forces a background damping coefficient k_{h}, which is independent of the particle's contact situation is applied to improve system stability. After contact detection and calculation of the corresponding contact reactions, the equations are integrated by a semi-implicit Newmark-Integrator scheme. As this method is unconditionally stable, larger time steps compared to explicit solvers are achievable ([7], [1]).

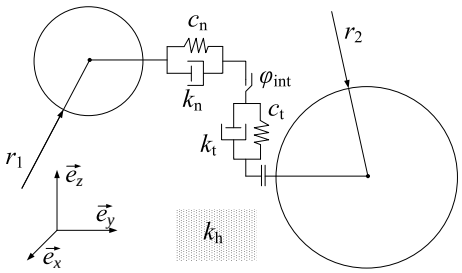

Figure 3. Interparticle contact model for normal and tangential direction

2.2. Modeling the grains shape

Grains in real soils are shaped by the process of their formation and wear. These shapes often consist of a high number of edges and are often non-convex. The particle's geometry strongly influences the rotational behaviour on micro-scale and thus the shear strength on macro-scale of the material (see also [25]). The common shape for DEM is a spherical particle. Spheres have no geometrical resistance torque against rotation, therefore high interparticle friction values are needed to gain sufficient shear strength.

Modeling the real particles shapes is possible using clumped spherical or single polygonal particles, but leads to much higher computational effort. As these geometries are not always convex, there is a possibility to have more than one contact point per particle pair. As computation time scales with the number of contacts n_{c} in a nonlinear manner, these shapes are not suitable for efficient simulation models.

A more effective way of modeling the grains rolling behaviour, is to add resistive torque laws to the contact

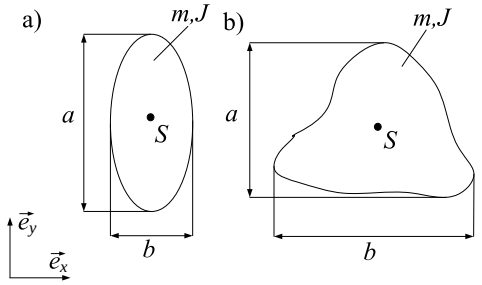

Figure 4. Aspect ratio as two dimensional parameter for two different grain shapes

model. Common resistance torque models are damping [1] or rotational velocity scaling strategies [28] and elastic torques with plastic limitation ([25], [26], [27]).
Strategies depending on the rotational velocity are not sufficient for quasi-static and static load cases as they are introducing a resistance to dynamic loads only. Elastic resistance torques are increasing the static shear strength, but are not covering the tilting behaviour of angular grains. Their torque rises to the plastic maximum from zero with increasing rotation, whereas the resistance torque due to tilting motion starts at its maximum torque (Figure 5 left position), which is decreasing (Figure 5 right position) and changing sign while tilting.
Therefore a new rotational contact model is currently developed. This model is mapping the tilting behaviour of arbitrarily shaped grains to computational efficient spherical particles (Figure 5). Thus the geometry of the particles is divided to the spherical body for contact detection and an additional two dimensional representation for every rotation around the particles local axis. Thus it is capable of reproducing anisotropic rolling behaviour by direction dependent elongation of the particle. As a first assumption rectangular geometries are used. To cover arbitrarily shaped grains, the aspect ratio angle γ is used. As shown in Figure 4 the aspect ratio angle γ can be defined as:

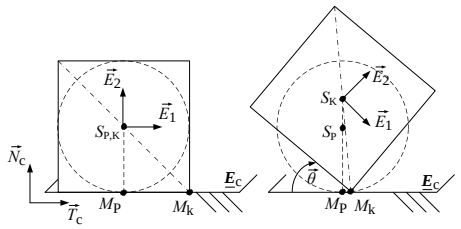

Figure 5. Mapping the grains rolling behaviour to spherical particle using nonlinear torque laws

$$\gamma = \arctan\left(\frac{a}{b}\right) \tag{6}$$

$$\gamma = \arctan\left(A\right) \tag{7}$$

$$\gamma \in \left(0; \frac{\pi}{2}\right)$$

where a and b are the dimensions of the grain and A is the aspect ratio. For each axis of rotation a corresponding rotation plane is defined, whereas the axis is the planes normal vector. From this plane and the contact plane $\underline{E}_c$ of both particles the normal and tangential force directional vectors ($\vec{N}_C, \vec{T}_C$) in the rotation plane could be derived. As the sphere rotates against another sphere, the instantaneous center of rotation M_P as well as the center of mass S_P gain no translational movement. Hence the virtual rectangle's center of rotation M_k needs to be moved in $\vec{T}_C$ direction (Figure 5). On that account the sphere is not moved like its virtual rotation geometry, but the corresponding torques are applied.
To calculate the torques, tangential as well as normal forces acting on the particles are used:

$$\begin{aligned}\vec{M}_P = \sum_{i,j,k=1}^{3} \Big(& \vec{F}_T^{jk} \times \left[l_T^{jk}\left(\theta_i(t), \gamma_i\right) \cdot \vec{N}_c^{jk} \right] + \\ & \vec{F}_N^{jk} \times \left[l_N^{jk}\left(\theta_i(t), \gamma_i\right) \cdot \vec{T}_c^{jk} \right] \Big) \\ i,j,k = & [1,2,3] \wedge i \neq j \neq k\end{aligned} \tag{8}$$

where i is the actual axis of rotation and l_T, l_N are the nonlinear moment arms for the respective forces, which are dependent on $\theta_i\left(t\right)$ as well as γ_i. The forces acting in the rotation plane need to be derived from the particles contact forces by projection from $\mathbb{R}^3$ in the corresponding $\mathbb{R}^2$ of the plane. The rotation angle θ_i around each axis is calculated from the local particle coordinate system and the contact plane each time step.
The proposed torque law covers the tilting behaviour of angular grains. Therefore only one additional parameter γ is introduced, which is connected to physical grains shape.

2.3. Parameter estimation

The estimation of the micro-scale parameters is still an unsolved issue in DEM simulations. Common strategies are comparing real and simulated material tests, while optimizing the contact model parameters using the error as criterion. The downside of this strategy is the high amount of iterations needed to gain sufficient parameters. Additionally these strategies are only delivering parameters for one special soil.
To estimate the parameters in an efficient way, a strategy that lowers the number of iterations to a minimum is used. This is done by reducing the number of arbitrary parameters. Therefore the parameters are stored in a parameter matrix $\underline{\Lambda}_P$, such that:

$$\underline{\Lambda}_P := \begin{pmatrix} E, \nu & k_N & r & 0 & \rho \\ c_T & k_T & 0 & \phi & 0 \\ 0 & 0 & r & \gamma & J \end{pmatrix} \tag{9}$$

wherein the lines are corresponding to the direction (normal, tangential and rotational) and the columns are corresponding to stiffness, damping, geometry, shear and inertia parameters. Some of these parameters can be obtained analytically by modeling constraints in advance.
Preliminary analysis studying the parameter influence on

piling processes and bevameter measurements were carried out. It could be shown, that the particles stiffness is mainly concerning the elastic behaviour of the system (as shown in [29], too). Higher stiffness values are causing higher computational effort and numerical problems, as the eigenfrequency of a particle pair is rising accordingly. Due to soils mainly plastic deformation and dissipative characteristics the stiffness can be decreased.

A systematic approach is used to calculate the particles

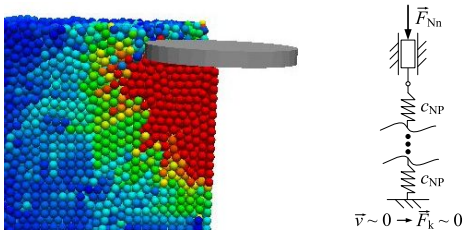

Figure 6. Equivalent model (r.) for minimum stiffness calculation using bevameter simulation (l.)

stiffness before simulation. The stiffness needs to be sufficiently high to avoid large overlaps. Therefore it can be calculated using the maximum allowed overlap. Assuming the worst case of a cubic primitive lattice packing, the minimum stiffness c_{n} for bevameter test simulations can be derived as:

$$c_{\mathrm{n}} \geq 2\pi z_{\mathrm{h}} \frac{3\vec{p} \cdot \frac{R}{r} + z_{\mathrm{h}} \cdot \rho_{\mathrm{p}} \cdot \vec{g}}{3\vec{a}} \qquad (10)$$

$$a = \frac{\delta}{r} \quad |a| \leq a_{\max}$$

thereby $\vec{p}$ is the expected soil pressure (from experiments) and z_{h} is the height of the simulation domain, corrected by the expected sinkage. R and r are the bevameter plate's and particle's radii. The calculated stiffness is used to choose Young's modulus for the Hertzian model based on equivalent linear stiffness. Poisson's number is then chosen dependent on the used material's properties. In [30] an overview of contact parameters for DEM is shown. For the presented range of the tangential stiffness from $c_t = 0,05..1 \cdot c_n$ almost no influence has been observed in the preliminary analysis. As a lower boundary $c_t = 0,03 \cdot c_n$ was discovered. For reduction of calculation time the lowest value is used. The damping values are chosen to be a fraction of the critical damping k_{krit} for the particle pair with the highest eigenfrequency. It is chosen as a compromise between stability and establishing of steady state conditions dependent on the load case (e.g. wheel or pressure-sinkage simulation). Thereby damping is in a range of $k = 2..15\% \cdot k_{\mathrm{krit}}$. Due to limited computation power and time it is not possible to assign the real soils grain size as particle radius. A common procedure is to scale up the particle size. To perform the scaling in a reproducible way, the resolution Γ is introduced as:

$$\Gamma = \frac{L_{\min}}{2r_{\max}} \qquad (11)$$

where $L_{\min}$ is the smallest dimension of the tool manipulating the soil (e.g. grouser length, bevameter plate) and $r_{\max}$ the biggest particles diameter. By using the resolution Γ to choose the particle size, it is assumed that for sufficiently high $\Gamma \geq \Gamma_{\min}$ enough particles are manipulated at the same time to cover the soil deformation effects introduced by the tool.

It has been observed that for $\Gamma \geq 2..3$ there is low influence of the particles radius for wheel simulations. In [19] similar resolution ($\Gamma = 1.25..5$) is used. For bevameter and piling simulations the resolution should be $\Gamma \geq 10$. The particles density is set to the according materials values. The inertia of the particles is dependent on its geometric properties and density:

$$J_i = \frac{1}{9} \cdot \pi \rho r^3 \left(\frac{r}{A_i} \right)^2 \qquad (12)$$

It is assigned as an anisotropic parameter depending on the axis of rotation, to meet the virtual elongated particle rotation geometry. The friction angle between the tool (e.g. wheel surface, bevameter plate) and particles is measured by bevameter shear tests using plates without grousers but similar tool material.

The main influencing parameters for shear strength are ϕ and γ/A. Thus they need to be chosen according to experimental data. It is planned to create lookup tables for a variety of values, which enables the selection of these parameters from real soil values without the need of preliminary calibration simulations.

For a first verification of the DEM soil modeling and the proposed parameter mapping method, the bevameter test is carried out in reality as well as in simulation. Figure 7 shows the pressure sinkage relation for both measured and computed test for a milled lava sand (RMC-Soil03) with a friction angle of $\psi = 31°$.

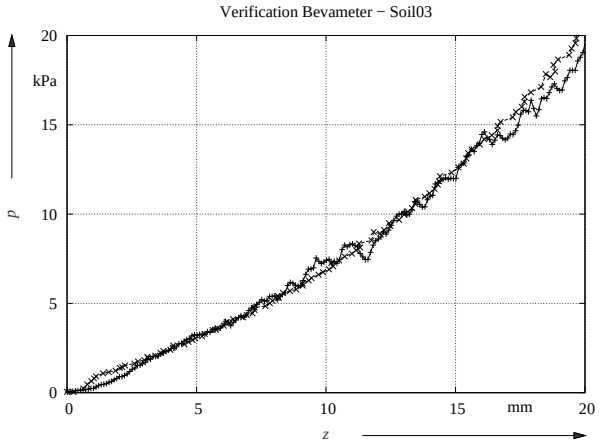

Figure 7. pressure sinkage test carried out as simulation (+) and measurement (×)

3. ANALYSIS OF WHEELED ROVER LOCOMOTION

3.1. Model setup

The DEM model for single wheel simulation consists of a particle filled soil bin and the wheel's representation. The boundaries as well as the wheels are represented by triangulated surfaces. The wheel surface is created by parametric equations and imported to Pasimodo. Figure 8 shows some examples for wheels that can be created using this approach. The triangulated wheel is attached

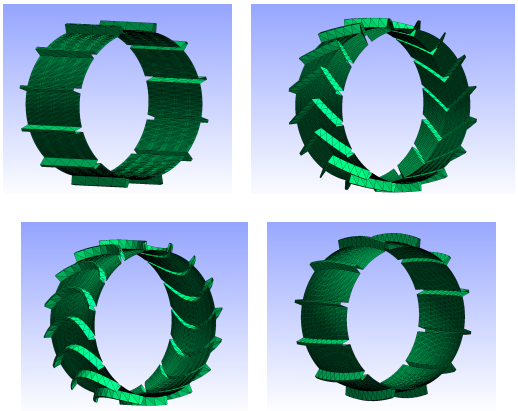

Figure 8. Examples for the output of the analytical wheel creation

to a non-contacting particle which is calculating its dynamics based on the summed contact reactions (Figure 1). To reduce the computation time mirror symmetry is used to simulate only half the number of particles. The symmetry boundary is modeled as frictionless wall, as it can be assumed that neighboring particles would have the same velocity and load state as the particles contacting the boundary.

The proposed single wheel DEM model is executed in

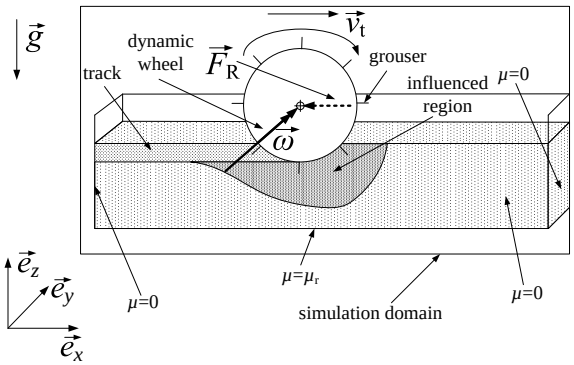

Figure 9. Model setup for single wheel test simulations

three steps by the wheel simulation framework. At first the particles are dropped into the soil bin. This step needs to be executed only once per soil setup. As a second step the wheel is dropped into the soil, while its rotational DoFs are locked. After steady state sinkage is reached the simulator is stopped and the results (e.g. particle packing, wheel position) are forwarded to the driving simulation by the framework. Using the pre-computed static sinkage, a constant rotational velocity is assigned to the wheel and its steady state slippage is used to compare the locomotion performance of different setups. Additional resistance forces $\vec{F}_R$ can be applied to the model. A summary of the used parameters is shown in Table 1.

Table 1. Wheel simulation parameters

Parameter	
Wheel diameter	250 mm
Wheel width	125 mm
Grouser height	15 mm
Grouser number	0..28
Normal load	8,33 kg
Rotational velocity	$3\,s^{-1}$
Simulation domain	$1200 \times 200 \times 400\,mm^3$
Young's modulus	$3 \cdot 10^6 \frac{N}{m^2}$
Poisson's ratio	0.2
Particle density	$2400\,kg/m^3$
Resolution Γ	3
Maximum time step	$5 \cdot 10^{-5}s$
Number of particles	62000

3.2. Simulation results

As a first example of the capabilities of the model, simulations for Exomars sized wheels ($d_{wheel} = 250\,mm$) are carried out. Figure 10 shows the comparison of the real rovers wheel and the simulated one with 12 grousers. As wheels are modeled without side faces (Figure 8) to allow displaced soil to flow inside, the same effect occurring in reality is covered, but leading to few particles being "trapped" at the inner faces of the grousers. The formation of bumps from displaced soil can be observed in the model and are dependent on the grouser number and geometry.

Figure 11 shows the development of the force in travel

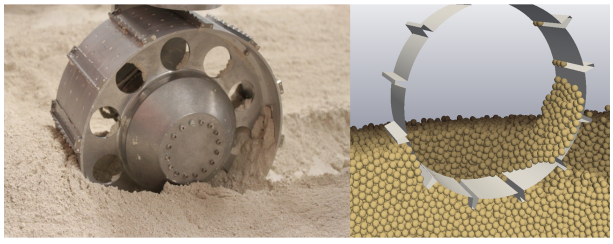

Figure 10. Rover wheel and single wheel simulation snapshot

direction for a wheel traveling through the soil. It can be seen, that steady state conditions are reached after $\approx 0{,}5\,m$. From recorded slip data it can be calculated,

that steady state is reached after 1,15 wheel revolutions are done. After reaching steady conditions the slip value is around 38%.
The steady state force in travel direction is fluctuating due to the changing number of grousers, which are currently manipulating the soil. In steady state either 6 or 7 grousers are manipulating the soil at once. To predict the

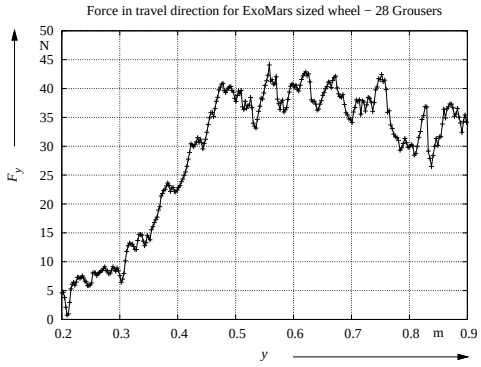

Figure 11. Force in travel direction for 28 grousers

the influence of the grouser number on the locomotion performance a parameter variation has been performed. Therefore the mean slip-value after gaining steady state condition is used as criterion for the tractive performance. To predict the influence of their number, the grousers need to be the main tractive elements of the wheel. To assure this, a rather large grouser height of 15 mm is used. By setting $\Gamma = 3$ the soils particles are assumed to be small enough to reproduce the grouser-effects.
As it can be seen in Figure 12, that for wheels with up to 20 grousers slip is reduced. Using more then 20 grousers shows almost no additional benefit in terms of locomotion performance, while torque is increasing with the number of grousers.

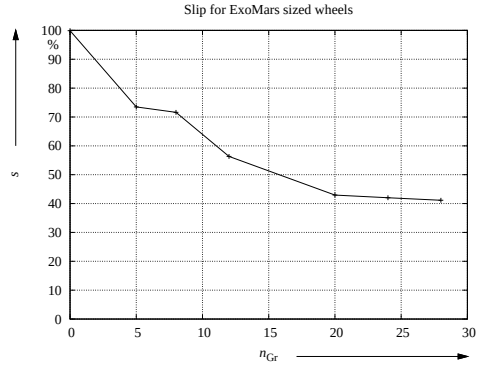

Figure 12. Steady state wheel slip dependent on the number of grousers

3.3. Further applications

The proposed DEM soil interaction model could not only be used to model wheeled locomotion on planetary surfaces. A first feasibility study modeling the HP^3-Mole's (Heat Flow and Physical Properties Package) hammering motion into the surface of Mars has been conducted for NASA's InSight Mission. With this first two dimensional model (Figure 13 (r.)) of the HP^3-Mole it could be shown that the DEM model is applicable for this kind of locomotion, too.

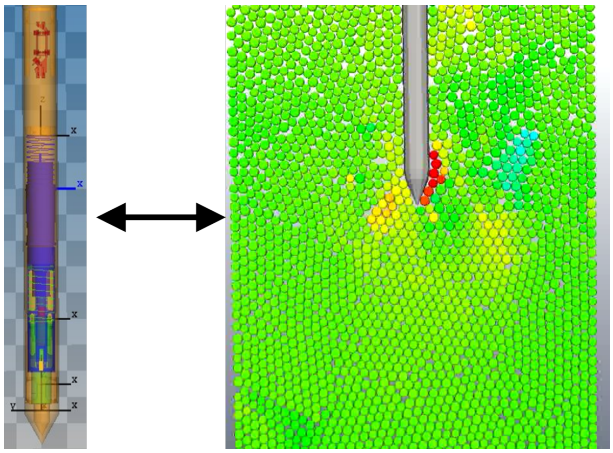

Figure 13. Optimization of HP^3-Mole using Multibody (l.) and Discrete Element (r.) approach

Because of the complex behaviour of the hammering mechanism, multibody models regarding inner contact dynamics are used to model it. As the soil has a big influence on the mole's performance, a currently used empirical soil model will be replaced by the DEM model. Therefore a co-simulation approach interconnecting both multibody and discrete element simulator will be used to carry out further optimizations of the mole (e.g. outer shape, tip angle etc.).

4. CONCLUSION

To improve the performance prediction of planetary rover wheels on soft soils a three-dimensional DEM model was developed. To estimate the micro scale parameters a new strategy using no preliminary calibration simulation is proposed and used for the simulation runs. To cover the angular shape of the grains, a new torque law using spherical particles is proposed. It was shown that the DEM model is applicable to wheel-soil interaction problems. A verification was performed by comparison of bevameter measurement and simulation. Further effects, like the formation of bumps from displaced soil as well as soil flowing into the open wheel geometry, occurring for real rover wheels driving through soft soil have been observed by the model. Single wheel measurements will be carried

out providing further validation.
It has been shown, that if a maximum number of grousers per wheel is exceeded, no further improvement of locomotion performance is occurring. It is planned to use the model for systematic analysis of wheel-soil interaction and planetary rover wheel development. As a second type of locomotion, the hammering into the martian surface has been modeled for the HP^3-Mole using DEM. A co-simulation of the hammering mechanisms multibody system and discrete element soil is under current development.

REFERENCES

[1] Fleissner, F., Pasimodo v1.9.3: software package and template files, Inpartik & ITM University of Stuttgart, Tübingen, 2012

[2] Bekker, M.G., Introduction to Terrain - Vehicle Systems, University of Michigan Press, Ann Arbor, 1969

[3] Wong, J.Y., Terramechanics and Off-Road Vehicle Engineering, Elsevier Ltd., Amsterdam, 2010

[4] Orr, M.K., Development of a finite element model to predict the behavior of a prototype wheel on lunar soil, Dissertation, Clemson University, 2010

[5] Krenn, R.; Hirzinger, G., SCM - A soil contact model for multi-body system simulations, 11th European Regional Conference of the International Society for Terrain-Vehicle Systems - ISTVS 2009, 2009, Bremen

[6] Pruiksma, J. P.; Kruse, G. A. M.; Teunissen, J. A. M.; van Winnendael, M. F. P., Tractive performance modelling of the Exomars rover wheel design on loosely packed soil using the coupled eulerian lagrangian finite element technique

[7] Willner, K., Kontinuums- und Kontaktmechanik, Springer-Verlag, Berlin, 2003

[8] Cundall, P. A.; Strack, O. D. L., A discrete numerical model for granular assemblies, Geotechnique, 1979, 29, 47-65

[9] Obermayr, M.; Dressler, K.; Vrettos, C.; Eberhard, P., Prediction of draft forces in cohesionless soil with the Discrete Element Method, Journal of Terramechanics, 2011, 48

[10] Coetzee, C. J.; Els, D. N. J., Calibration of granular material parameters for DEM modelling and numerical verification by blade-granular material interaction, Journal of Terramechanics, 2009, 46

[11] Coetzee, C. J.; Els, D. N. J.; Dymond, G., Discrete element parameter calibration and the modelling of dragline bucket filling, Journal of Terramechanics, 2010, 47

[12] Kanou, S.; Amano, M.; Terasaka, Y.; Matsumoto, N.; Wada, T., Terra-Mechanical Simulation Using Distinct Element Method, Komatsu Vol.49 No.151, 2003

[13] Tsuji, T.; Nakagawa, Y.; Matsumoto, N.; Kadono, Y.; Takayama, T.; Tanaka, T. 3-D DEM simulation of cohesive soil-pushing behavior, Journal of Terramechanics, 2012, 49

[14] Mishra, B. K. A, review of computer simulation of tumbling mills by the discrete element method, Part 1 - contact mechanics, Int. Journal of Mineral Processing, 2003, 71

[15] Johnson, J. B. et.al., Determining Mars soil properties from laboratory tests, discrete element modeling and Mars trenching experiments, Seventh International Conference on Mars, 2007

[16] Knuth, M.; Johnson, J.; Hopkins, M.; Sullivan, R.; Moore, J., Discrete element modeling of a Mars Exploration Rover wheel in granular material, Journal of Terramechanics, 2011

[17] Li, W.; Huang, Y.; Cui, Y.; Dong, S.; Wang, J., Trafficability analysis of lunar mare terrain by means of the discrete element method for wheeled rover locomotion, Journal of Terramechanics, 2010, 47

[18] Nakashima, H.; Oida, A., Algorithm and implementation of soil-tire contact analysis code based on dynamic FE-DE method, Journal of Terramechanics, 2004, 41

[19] Nakashima, H.; Oida, A.; Momozu, M.; Kawase, Y.; Kanamori, H., Parametric analysis of lugged wheel performance for a lunar microrover by means of DEM, Journal of Terramechanics, 2007, 44

[20] Nakashima, H. et.al., Discrete element method analysis of single wheel performance for a small lunar rover on sloped terrain, Journal of Terramechanics, 2010, 47

[21] Wakui, F.; Terumichi, Y., Numerical simulation of Tire-Ground System Considering Soft Ground Characteristics, Journal of System Design and Dynamics, 2011, 5 No.8

[22] Ergenzinger, C.; Seifried, R., Eberhard, P., A discrete element model to describe failure of strong rock in uniaxial compression, Granular Matter, 2011

[23] Chevalier, B.; Combe, G.; Villard, P., Experimental and discrete element modeling studies of the trapdoor problem: inuence of the macro-mechanical frictional parameters, ACTA Geotechnica, 2012

[24] Vetsch, D., Numerical Simulation of Sediment Transport with Meshfree Methods, Technische Hochschule Zuerich, 2012

[25] Oda, M.; Iwashita, K., Study on couple stress and shear band development in granular media based on numerical simulation analyses, International Journal of Engineering Science, 2000

[26] Rojek, J.; Zarate, F.; Agelet de Saracibar, C.; Gilbourne, C.; Verdot, P., Discrete element modelling and simulation of sand mould manufacture for the lost foam process, International Journal for Numerical Methods in Engineering, 2005

[27] Plassiard, J.-P.; Belheine, N.; Donze, F.-V., Calibration procedure for spherical discrete elements using a local moment law, University Grenoble, 2007

[28] Wu, W., Modellierung von Massenbewegungen: Stand der Technik und neue Entwicklungen, Institut für Geotechnik, Universität für Bodenkultur, Wien, 2010

[29] Plassiard, J.-P.; Belheine, N.; Donze, F.-V., A spherical discrete element model: calibration procedure and incremental response, Granular Matter, 2009

[30] Khot, L. R.; Salokhe, V. M.; Jayasuriya, H. P. W.; Nakashima, H., Experimental validation of distinct element simulation for dynamic wheel-soil interaction, Journal of Terramechanics, 2007, 44